Study of the angular correlation of the gamma radiation emitted following β^- decay of ^{60}Co

Physics laboratory - 29/10/2023
Group 3
Marchesini Davide - 2121242
Lorenzo Frigato - 2109747
Aneesh Suresh Nene - 2004982

1 Abstract

In a nuclear gamma-gamma cascade, the radiation emitted is not isotropic, as can be theoretically predicted, but its angular distribution changes depending on how the spin of the nucleus is oriented in space. This property can be used, for example, to study the fundamental properties of nuclear interactions, and it is a predominant field for nuclear model research. In this experiment we want to study the correlation in the angular distributions of the two gamma rays emitted, following the β^- decay of ^{60}Co. For this reason, our aim is to also provide a proper calibration and study the efficiency of the two NaI scintillator detectors used in the laboratory, through the modelling of their geometry and the investigation of any source of possible systematic errors.

2 Experimental setup

The first detector (Detector 1) is fixed, while the second one (Detector 2) can rotate with an angle θ with respect to the axis defined by the first detector, as shown in figure 1. Both detectors lie in the same plane and can vary their distance from the source of ^{60}Co, which is located in the axis of rotation of the two detectors. This distance has been kept fixed at d_1=12 cm and d_2=22 cm. It is indeed important that the source lies exactly in the axis of rotation of the two detectors, because a small misplacement could introduce systematic errors in the measurement of the angular correlation. These errors can also be taken into account considering the physical size of the source, that is usually considered in a first approximation, as point-like. A scheme of the apparatus is provided in figure 1.

Both detector are then connected to a Quad Linear Gate FAN-IN-FAN-OUT. The signal for each detector is therefore doubled. For each detector, a copy of the signal is sent directly into a CAEN digitizer for data acquisition, while the other copy is first sent to Constant Time Fraction Discriminator (CFD), and then to a Coincidence Logic Unit to provide the trigger for the data acquisition of the digitizer. The latter allows two possible logical operation: OR and AND. The CFD allows us to change some parameters of the signal, such as its delay and width value. This is essential to achieve an overlap of the signals coming from the two detectors, and then measure events in coincidence.

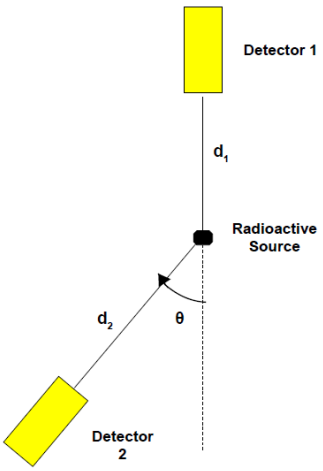

Figure 1: Experimental set-up

3 Data analysis

3.1 Preparation and calibration of the detectors

To acquire meaningful data, it is necessary to properly set up the experimental apparatus and perform an energy calibration of the detectors. In this case we set a CFD threshold to cut out the electric noise of the apparatus. The threshold was set for both detectors through a trimmer, using an oscilloscope to make sure we did not miss low-energy events such as retro diffused photons. Consequently we can perform a calibration of the acquired spectrum, converting it from the DAQ arbitrary unit (ADC Analog to Digital Converter units) in energy (keV). A linear response of the detector is assumed

$$E_\gamma = N_{ADC} \cdot b + a \tag{1}$$

allowing us to properly calibrate our data. Therefore the following procedure was followed for both detectors. We acquired a spectrum for the ^{60}Co and one for the ^{241}Am, in order to gain accuracy in the low energy region. We then performed Gaussian fits over the peaks in order to derive the position of the peak. Then, a linear fit was executed, to find the b (angular coefficient) and a (offset) of the calibration. The experimental known values E_γ of the peaks were retrieved from the National Nuclear Data Center (NNDC) online data service [1]. We have shown an example of an acquired spectrum (figure 2) and of the linear calibration fits performed (figure 3). The results of the Gaussian and linear fits are shown in the tables 1 and 2.

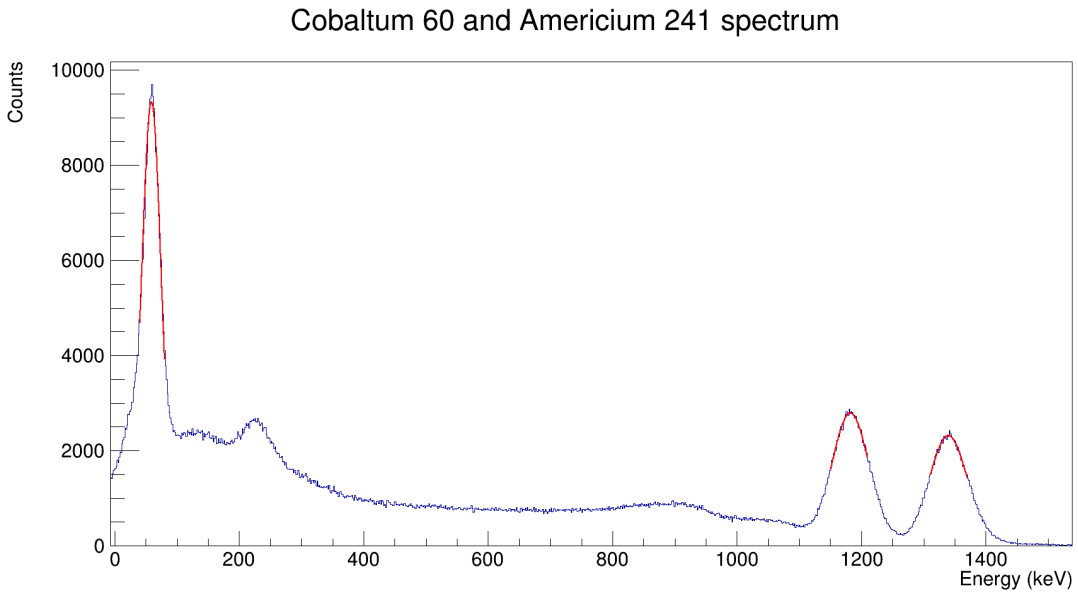

Figure 2: An example of an acquired spectrum in the laboratory for a 3 minute run. In this case, both the Americium and the Cobalt source were present, so it is possible to see the three peaks that are fitted through the Gaussian function.

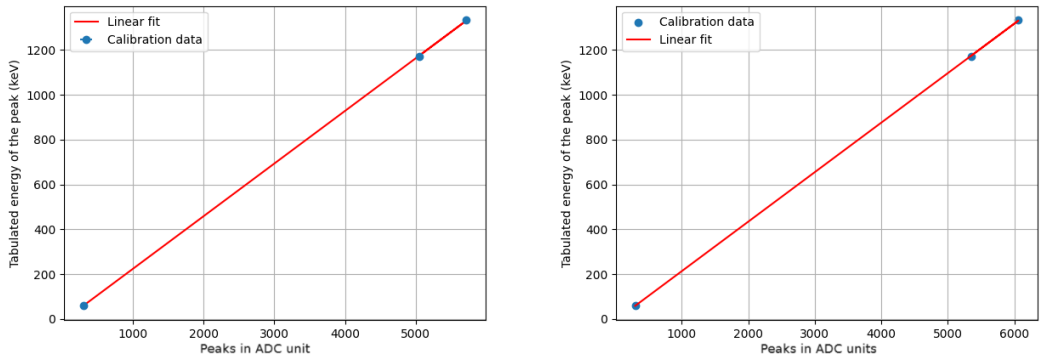

Figure 3: Calibration fit for the first detector (right) and for the second detector (left).

Source	Energy (Kev)	Detector 1		Detector 2	
		Mean [ADC]	Sigma [ADC]	Mean [ADC]	Sigma [ADC]
Co 60	1173	5045.2 ± 0.4	118.6 ± 0.5	5354 ± 1	127 ± 2
Co 61	1333	5724.6 ± 0.5	124.5 ± 0.6	6063 ± 1	142 ± 1
Am 241	59	291.6 ± 0.1	29.1 ± 0.1	300.0 ± 0.3	68.0 ± 0.6

Table 1: Gaussian fit results on the spectrum peaks (expressed in Analog to Digital Converter unit - ADC) for the calibrations of detector 1 and detector 2

	b [keV/ADC]	a [keV]
Detector 1	0.2344 ± 0.0005	-9 ± 2
Detector 2	0.2209 ± 0.0005	-7 ± 2

Table 2: Results of the linear fits for the calibration of both detectors.

Since the photo-peak position can be obtained from a Gaussian fit on the experimental histogram, it is appropriate to investigate how the precision, with which we are able to determine the peak position through the fit, varies with the number of events acquired, and so the corresponding measurement accuracy. For this purpose, several acquisition were plotted, varying the number of acquired events: 500, 1000, 2000, 5000, 10000, 100000. Due to the efficiency of the detectors and the randomness of the energy collected by the detectors during each event, we can describe the photo-peaks as Gaussian. It is well known that the error of the mean of a Gaussian variable (the energy of the peak in this case) follow the proportionality

$$\sigma_{mean} \propto \frac{1}{\sqrt{N}}$$

where N is the number of the events collected. Furthermore, since the number of decays follows a Poisson statistic, we expect that the precision with which we are able to estimate the number of events in the peak, will be proportionate to

$$\lambda = \frac{\sigma}{\mu} \propto \frac{\sqrt{N}}{N} = \frac{1}{\sqrt{N}}$$

where N is the average number of decays in the unit of time (in this simple estimate we neglect the efficiency of the detector, which will be taken into account, properly, later), and μ and σ^2 are the medium and the variance of this distribution. Indeed, fitting over the 1333 keV peak one finds that the error of the mean decreases with the number of acquired events, as expected (figure 4).

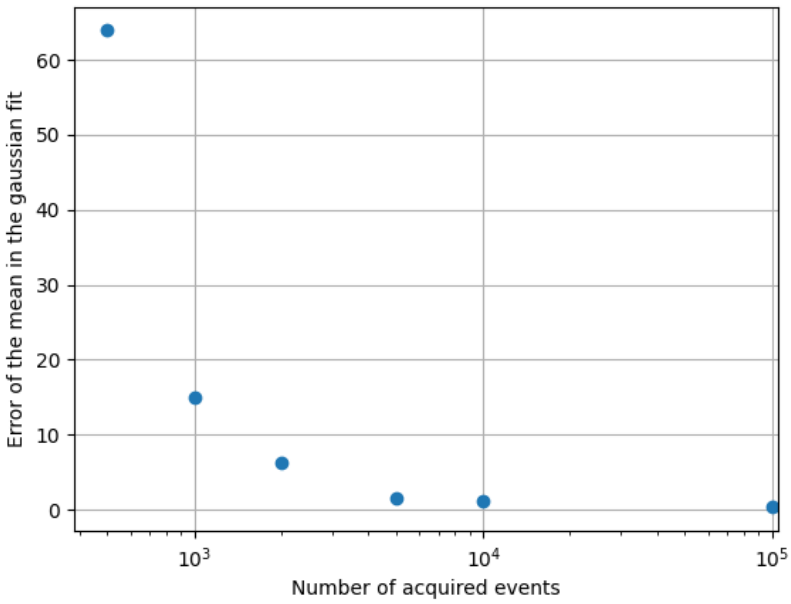

Figure 4: Number of acquired events over the mean's error after a Gaussian fit over the peak. Notice that the x-axis is in logarithmic scale.

Ultimately, the software used to interface with the data acquisition, VERDI, allows us to change the integration time used by the DAQ, namely the long gate. Varying it, could result in a optimization in the peak resolution. A series of runs of 1 minute each were taken for both detectors in order to find the best value for the long gate fitting on the 1333 keV peak to find its position and FWHM.

	Detector 1			Detector 2		
Long Range	Centroid (keV)	FWHM (keV)	R	Centroid (keV)	FWHM (keV)	Resolution
250	1277	71.65	5.61%	1255	66.44	5.29%
300	1347	74.69	5.54%	1322	69.39	5.25%
350	1384	78.06	5.63%	1356	71.69	5.28%
400	1401	79.85	5.69%	1377	71.69	5.20%
450	1414	82.97	5.86%	1390	75.38	5.42%
500	1425	82.91	5.81%	1399	76.53	5.47%
550	1431	85.63	5.98%	1405	78.18	5.56%
600	1438	91.613	6.37%	1408	81.02	5.75%

Table 3: Centroid of the 1333 Kev peak and its FWHM for different values of the integration time

3.2 Background measurement

We present a comprehensive background measurement conducted over a duration of 24 hours. The purpose of this extended measurement is to enhance the accuracy of subsequent data analyses. The acquired background data is essential for a precise determination of the number of counts associated with events of interest, particularly critical for accurate measurements for the efficiency. The forthcoming data analysis will involve the subtraction of the background from the primary data-set to account for the correct number of events. A detailed spectrum of the background is presented in the figure 5. Notably, the spectrum reveals a low-energy Compton continuum, attributable to photons coming from other radioactive sources within the laboratory environment, or natural sources. Additionally, the background spectrum encompasses contributions from secondary cosmic rays. It is noteworthy that, although high-energy events are less frequent, their significance in the overall context of the study is not to be dismissed, particularly around $2500keV$, as it will be shown later.

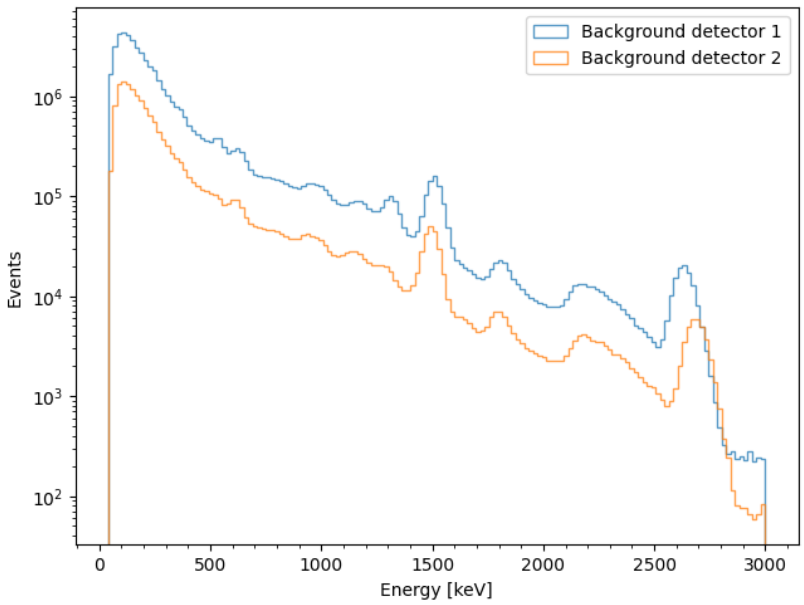

Figure 5: Background spectrum during a 24h-long acquisition. Please note that the y-axis is in log scale.

NOTE: During the initial two days of data acquisition, many parts of the experimental apparatus were found to be malfunctioning. We managed to detect and correct most of them, in time, during live data analysis (for example, a CFD output was found to be malfunctioning). Unfortunately, until the third day,

we were unable to detect one of the malfunctions, where the problem was identified and rectified by Professor Simi. A cable carrying the output of the detector 1 signal from the CFD to the logic unit was found to be broken: either the electrodes were not making contact or, more likely, something was broken inside it. As a result, sometimes the data acquisition, especially in the AND configuration, do not acquire events, because the cable from detector 1 wasn't carrying any signal. This would happen only if the cable was disturbed. So, in theory, since the data acquisition was made from the computer terminal without touching the apparatus except maybe for a few brief moments, the number of counts shouldn't have been affected too much. Anyway, after changing the cable, the number of counts significantly increased at parity of time of observations, which means that the hypothesis that this do not affect the data too much is no longer true. The correct thing to do would be to retake the experimental data,but since there was no time due to the strict laboratory schedule for all the groups, this has not been done. The analysis of the data is performed anyway, taking into account that this signal transmission problem has affected equally the number of events acquired in this way. Importantly we do need only to compare measurement of total counting and if all the data are affected equally this does not change our results significantly.

3.3 Research and characterization of systematic errors

The number of events acquired by both the detectors can change due to the presence of systematic errors in the experimental apparatus. The displacement of the source from the rotational axis of the detectors is indeed one of them, and could lead to a systematic error in the number of counts expected, which depends on the angle θ between the detectors. If one wants to do the angular correlation measurements, this must be corrected. For this purpose a series of runs of 5 minutes each were taken at various angular configurations (θ= 0, 20, 40, 50, 70, 90 degrees) in a OR configuration. Given that the detector logic configuration is set in OR we can assume that the radiation emitted by the source is isotropic, because we are not measuring correlation between the two gammas (AND configuration). Given that the detector cover a finite solid angle one expect (refer to the scheme in figure 6) that the number of counts in the unit of time N for the detector 2 is

$$N_2(\theta, d) = \frac{N_{emitt}\Sigma}{4\pi(d_2^2 + d^2 + 2d_2 d sin(\theta + \psi))} \tag{2}$$

where d is the displacement from the source, N_{emitt} is the number of emitted particles in the unit of time from the source, Σ is the area of the detector and ψ the angle from the arbitrary horizontal axis chosen in Fig 6. Notice that if $d = 0$ one recover the ideal situation and its expected number of counts that does not depend on θ. Since $\xi = N_{emitt}\Sigma$ is just a normalization factor, one can fit the number of events collected by the second detector in function of θ with equation 2 to find the two parameter of interest, d and ψ. Hence this systematic error can be taken into account by defining a correction function

$$f_{corr} = \frac{N_2(d=0)}{N_2(\theta, d)} = 1 + \frac{d^2}{d_2^2} + 2\frac{d}{d_2} sin(\theta + \psi) \tag{3}$$

To study the systematic errors in the detectors, we fit Gaussian curve on the second peak corresponding to the energy of 1333 keV. The area of the Gaussian integral given by $\sqrt{2\pi}A\sigma$ gives the estimate of total number of counts. Here, A is the constant given by the Gaussian fit and σ is the standard deviation also provided by the fit, along with the errors on both these parameters. To calculate the error in the number of counts, we used the formula:

$$\sigma_N^2 = \left[\sigma_A^2 \left(\frac{\partial N}{\partial A}\right)^2 + \sigma_\sigma^2 \left(\frac{\partial N}{\partial \sigma}\right)^2\right] \tag{4}$$

where, σ_N, σ_A and σ_σ are the errors corresponding to the number of counts, the constant and the standard deviation respectively. After estimating the number of counts in function of θ, we can fit the experimental data by the function given by equation 2. The results we obtained are given in figure 7. The obtained values for the parameters and theirs errors are given in the table 4. We did not plot the data for $\theta = 20^o$ because the file we obtained during the data acquisition was corrupted and could not be used. This also limited the neatness of our fit since we had 1 point in the data-set missing.

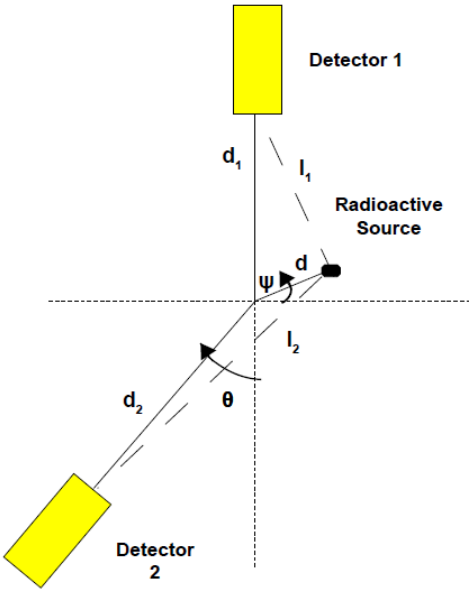

Figure 6: Deviation from the ideal set-up (refer to Fig 1) and the corresponding change in the geometry of the system

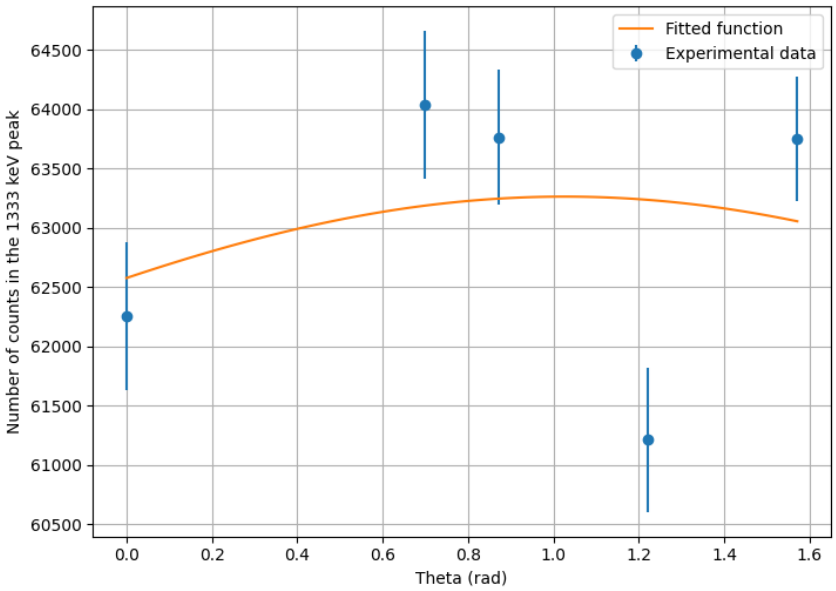

Figure 7: Number of measured events as a function of the angle to determine possible geometry systematic error.

Parameter	Value	Error
$N_{emitt}\Sigma$	$3.7 \cdot 10^8$	$2 \cdot 10^7$
d (cm)	0.2	0.9
ψ (rad)	2	1
χ^2	15.7	-

Table 4: Parameters obtained from the fit and their relative errors

As seen from the table 4, the value of the parameter d and its corresponding error are comparable, therefore we can consider that d is compatible with 0. We can safely set $d \approx 0$, and because of that the correction function will be $f_{corr} \approx 1$. We also observe the value of χ^2 is really far from the expected value for a CL

of 95% for 2 degrees of freedom, that is $\chi^2 = 0.10$. Thus, it can be concluded that the data we acquired was insufficient to confidently state to have been able to quantify the presence of systematic errors in the placement of the source.
Another source of systematic error is the so called dead-time of the DAQ, i.e the time window after an acquired event in which the DAQ doesn't acquire events. If the source is active and the rate of acquired events is high, we could lose significant events if they are revealed by the detectors in this time window. An estimate of the number of lost events due to dead time can be done confronting the acquired events from the DAQ and the counted events by the CAEN scaler. It is found that the number of events lost due to dead time is the 16.5% of the total events counted by the CAEN digitizer. A simple estimate of the dead time can be given if we suppose that there is a constant rate in which the nuclear decays (and so the events acquired) happen in time. This is the same as supposing a Poisson distribution of the latter. Dividing the observation time by the numbers of events acquired by both the CAEN and the DAQ one can find the average time in which one event happen, respectively τ_{CAEN} and τ_{DAQ}. Therefore, since know that this must be true

$$\tau_{CAEN} = \tau_{dead} + \tau_{DAQ}$$

we can easily estimate the dead time as

$$\tau_{dead} = \tau_{CAEN} - \tau_{DAQ} = 4.21 \cdot 10^{-5} s$$

This dead time seems too big to be the correct one, and probably it's because of the low rate of the events acquired due to the cable issue already discussed.

3.4 Measurement of detectors efficiency

To calculate the efficiency of the detectors we used two methods: the sum-peak method and the coincidence method. We will discuss them separately. First we need to define how we decided to count the events under a certain photo-peak. We will use the two Gaussian integrals $\sqrt{2\pi}A\sigma$ and $2\pi A\sigma_x\sigma_y$, respectively the integral of a one dimensional Gaussian, already used in the previous section, and the integral of a two dimensional circular Gaussian (which is $Aexp[-(x-\mu_x)/(\sqrt{2}\sigma_x) - (y-\mu_y/)(\sqrt{2}\sigma_y])$), with σ the standard deviation and A the normalization factor. In this way we perform our fit and calculate the number of events. To determine the counting from these two formulae, we have to divide for the bin size, while for the case of two dimensional Gaussian it must be the area of the bin, obtaining the real numbers N. Additionally, in the following analysis, to have meaningful results we will have to discriminate between the obtained experimental coincidences (or events in the sum-peak method) to pick only the significant ones. Therefore we define a *true coincidence* (or a *true event*, in the case of the sum.peak method) when we reveal two gamma rays in coincidence that were originated in the same nuclear decay. Vice-versa, we define a *random coincidence* (or a *random event*) when instead we reveal two gamma rays in coincidence that are coming from different nuclear decays.

3.4.1 Sum-peak method

In a first approximation, the probability of detecting both gammas (coming from the same nuclear decay) in the same detector is given by the product of the probabilities to reveal the individual gammas, where, since the photons are coming from the same nuclear decay, the angular correlation between the two must be taken into account. Therefore, from our calculation the efficiency for the two detectors is given by the equations :

$$\varepsilon_1(1173) = \frac{N_{2506}}{N_{1333}} \cdot \frac{\Omega_1}{C(0)} \qquad \varepsilon_1(1333) = \frac{N_{2506}}{N_{1173}} \cdot \frac{\Omega_1}{C(0)}$$
$$\varepsilon_2(1173) = \frac{N_{2506}}{N_{1333}} \cdot \frac{\Omega_2}{C(0)} \qquad \varepsilon_2(1333) = \frac{N_{2506}}{N_{1173}} \cdot \frac{\Omega_2}{C(0)}$$

with Ω, the geometrical factor is given by,

$$\Omega = \frac{4\pi d^2}{\pi r^2} = 4(\frac{d}{r})^2$$

where r is the radius of the detector and d the distance, and

$$C(0) = \frac{A(0)}{\int_0^{2\pi} A(\theta)d\theta} = \frac{(1 + \frac{1}{8} + \frac{1}{24})}{\int_0^{2\pi} A(\theta)d\theta} \approx 0.172$$

is the factor due to angular correlation. For the sum-peak we would have to look at one dimensional histogram and search for the peak $2506keV$ to get the number of events in which two different photons reached the same detector. Then, we have to discriminate and select only the true events. To quantify the number of random coincidence we could look at the $2346keV$ and $2666keV$ peaks, that are formed when two photon of the same kind (both 1173 keV or both 1333 keV) reached simultaneously the same detector. In a first approximation, the rate in which these events occur is the same in which the random events in the sum peaks occur. Estimating the number of these kind of events would therefore give an estimate of the number of random coincidences, allowing us to calculate the true coincidences and so the detector efficiency. But it is impossible to clearly define these two peaks. Even with the subtracted background this is not possible for our data set. An indicator of some hidden problematic is presented by the huge differences between the two spectrum in figure 8, where we should find similar histograms but this is not the case. We nonetheless report

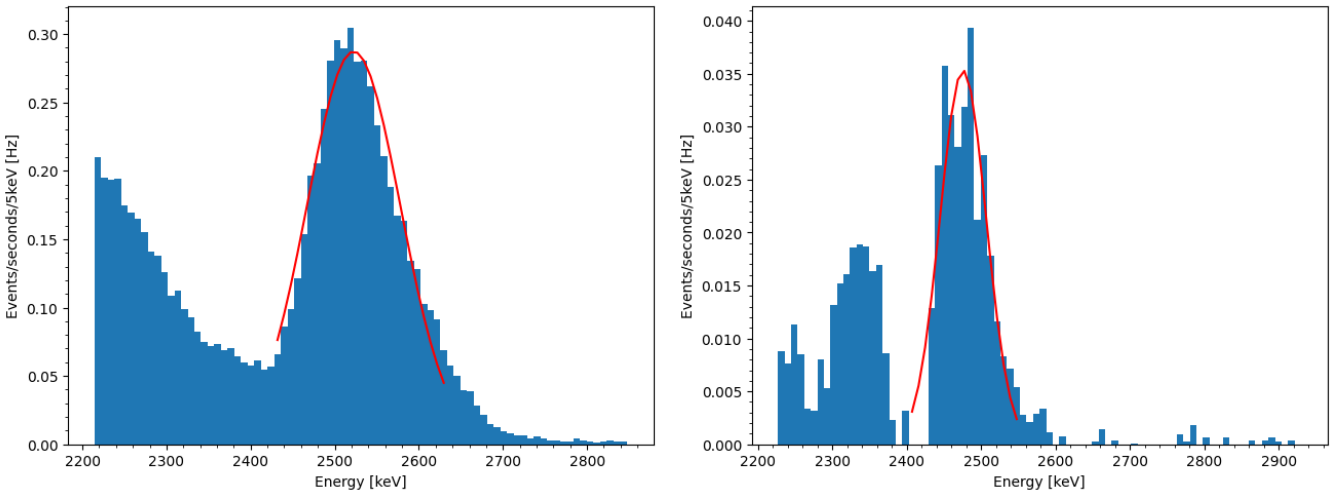

Figure 8: The histogram are the of events with the normalized subtracted background, with on the right the detector 1 and on the left detector 2.

in table 5 the results without the subtraction of the random coincidences, that are clearly non-physical.

	$\varepsilon_{1333}[\%]$	$\varepsilon_{1173}[\%]$
Detector 1	176 ± 5	148 ± 4
Detector 2	123 ± 10	103 ± 9

Table 5: Efficiency using the sum-peak method

3.4.2 Coincidence method

For the coincidence method we decided to perform two dimensional fit with a circular Gaussian to determine the number of events in coincidence where an AND condition is required. This has been done for the two regions, which are the two options

- photon 1333keV in detector 1 and photon 1173 in detector 2;
- photon 1333keV in detector 2 and photon 1173 in detector 1.

The formulas for the efficiency are then (as before the correlation between the two photons and the finite size of the detector must be taken into account)

$$\varepsilon_1(1173) = \frac{N(\gamma_1 \to detector1 \quad \gamma_2 \to detector2)}{N_{1333}} \cdot \frac{\Omega_1}{C(0)} \qquad \varepsilon_1(1333) = \frac{N(\gamma_1 \to detector2 \quad \gamma_2 \to detector1)}{N_{1173}} \cdot \frac{\Omega_1}{C(0)}$$

$$\varepsilon_2(1173) = \frac{N(\gamma_1 \to detector2 \quad \gamma_2 \to detector1)}{N_{1333}} \cdot \frac{\Omega_2}{C(0)} \qquad \varepsilon_2(1133) = \frac{N(\gamma_1 \to detector1 \quad \gamma_2 \to detector2)}{N_{1173}} \cdot \frac{\Omega_2}{C(0)}$$

where the term N_γ has already been calculated during the sum-peak method (with a one dimensional Gaussian fit). Without discriminating the random from the true coincidences as before, we get an efficiency

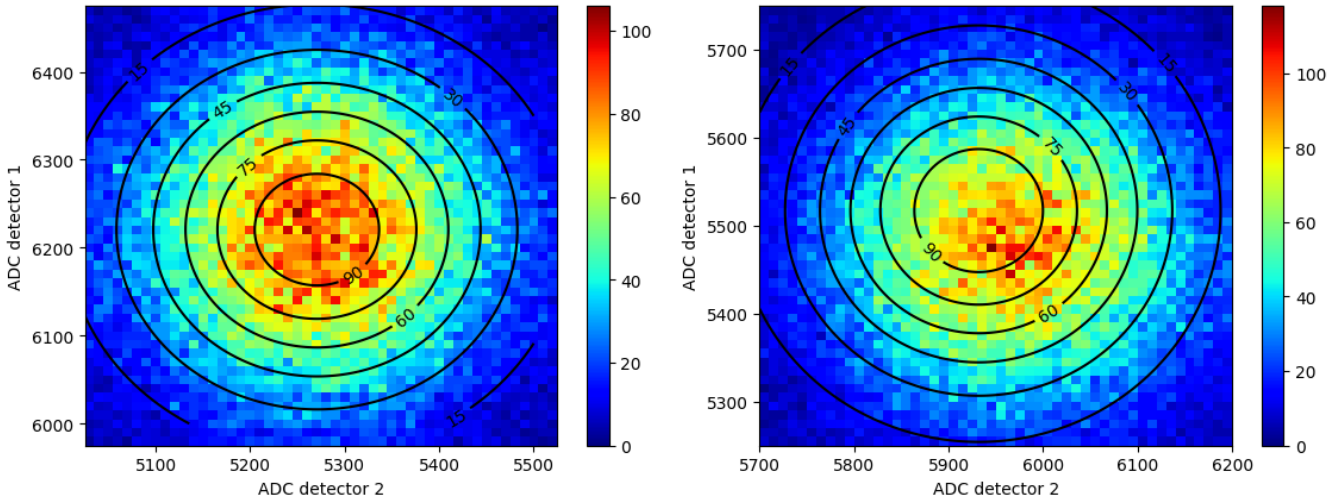

Figure 9: Two dimensional Gaussian fit for the region of interest, in black it is reported the contour levels of the Gaussian

over 100%. To fix this problem we need to remove the random coincidence events that cause this. To do so we need to calculate the events under the two peaks with the coincidence of two equal photons, which are of course random. For the coincidence method our random events number under on coincidence peak is supposed to be the mean of the two possible random events (the rate of occurrence of those random events is supposed to be equal for all possible configurations of photons)

$$N_{rand} = \frac{N_{\gamma_1,\gamma_1} + N_{\gamma_2,\gamma_2}}{2} \tag{5}$$

that were calculated performing two dimensional fit in that two regions, equal to what has been done in figure 9. We then substitute in the equations of the efficiency

$$N(number\ events\ for\ the\ region\ selected) \rightarrow N(number\ events\ for\ the\ region\ selected) - N_{rand} \tag{6}$$

In this case we were able to perform such operation, because now we are no more looking at the problematic region of the sum, but at the region with same x and y values. Executing all this operations for our data sets we get the results presented in the table 6. We can conclude confirming that our efficiency is indeed

	$\varepsilon_{1333}[\%]$	$\varepsilon_{1173}[\%]$
Detector 1	36 ± 3	32 ± 3
Detector 2	33 ± 2	26 ± 3

Table 6: Efficiency using the coincidence method

correct and in the range of the expected one for general NaI(Tl) scintillator.

3.5 Measurement of angular correlation

To estimate the angular correlation between two photons, we collected data by changing the angular position of detector 2 and imposing the condition AND in our electronics. We took several runs at various angular configurations (θ= 0, 20, 40, 50, 70, 90 degrees). In this way we collected events with real correlation but also random coincidences (as defined before), which are much less prominent than in the previous section. So, to remove the random coincidences we start by counting the events in the regions

$$\gamma_1 \rightarrow detector1 \quad \gamma_1 \rightarrow detector2$$
$$\gamma_2 \rightarrow detector1 \quad \gamma_2 \rightarrow detector2$$

founding the number of events N_1 and N_2. Hence, the random coincidences are given by $N_{rand} = (N_1+N_2)/2$, supposing that the rate of occurrence of those random coincidences is equal for all possible configurations of photons. Regarding the error of this measurement a Poisson distribution was considered, therefore the error

on the random coincidences is $\sqrt{N_{rand}}$.
In this case it was impossible to perform two dimensional fit to find the coincidences in the two peaks of interest (as we did before in the Coincidence method) because the number of events is much lower due to shorter observation time. Then, we selected events in the region $[1100keV, 1400keV] \times [1100keV, 1400keV]$, removing a lot of events that are not of interest (for instance, an event of the kind: $1173keV$ photon in the first detector and a photon of $500keV$ in the second one is not considered in our analysis). Successively we performed, with this selected events, one dimensional Gaussian fit in the spectrum of detector 2 in the two photo peaks, getting N_{γ_1} and N_{γ_2}, the number of events for the two photopeaks, like we did before multiple times in the previous sections. We then proceeded by subtracting the random coincidences: $N_\gamma(real) = N_\gamma - 2 \cdot N_{rand}$ with $\gamma = \gamma_1, \gamma_2$. The factor 2 is necessary because the counting performed with the latter fit counts the random coincidences with the same gamma (for instance $\gamma_1\gamma_1$) but also with different gammas ($\gamma_1\gamma_2$). Then we had to add the results for the possible coincidences combinations

$$\gamma_1 \to detector1 \quad \gamma_2 \to detector2$$
$$\gamma_1 \to detector2 \quad \gamma_2 \to detector1$$

which means that the total number of interesting events is $N = N_{\gamma_1}(real) + N_{\gamma_2}(real)$. In this way we found the number of total real coincidence events. Dividing by the number of events for the detector 2 in the configuration at 90°, we were are able to construct the variable $A(\theta)$ from our experimental data, getting the results presented in figure 10. With this data we performed a fit with the expected theoretical correlation function

$$A(\theta) = 1 + a \cdot cos^2(\theta) + b \cdot cos^4(\theta) \tag{7}$$

obtaining the results

$$a_{exp} = 0.13 \pm 0.05 \quad b_{exp} = 0.063 \pm 0.052$$

which as to be compared to the theoretical one, i.e. with $a_{th} = 1/8 = 0.125$ and $b_{th} = 1/24 \approx 0.042$. In the following figure we report our data but also the experimental fit and the theoretical prediction.

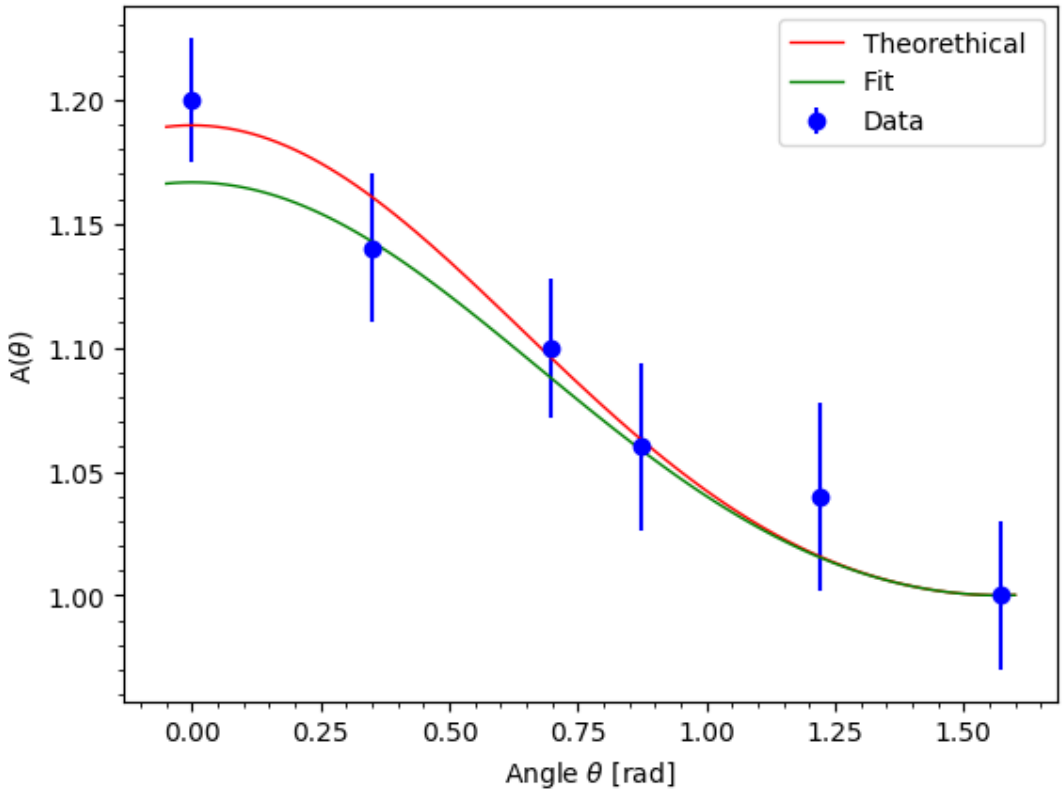

Figure 10: Experimental values for $A(\theta)$ plotted with the theoretical prediction and the experimental fit

4 Conclusion

In conclusion, we successfully set up the experimental apparatus finding optimal parameters for the calibration of our detector in energy and for the long gate. We've taken a 24h background measurement to eliminate possible noise and then we looked for possible geometrical systematic error cause by the fact that the source is not positioned in the axis of rotation of the two detectors. We were not able to find clear evidence of some misplacement in the position of the source. We decided also to study the efficiency of the scintillators with two methods: sum-peak method, which was unsuccessful because we were unable to find the other two important photo-peaks, and the coincidence method, which allowed us to determine a correct efficiency. In the end we collected data to prove the angular correlation between the two photons emitted by the Cobalt source, getting appropriate results. There were some difficulties regarding the electronics during the experiment and this influenced our data collections. This did not block us to do the analysis but it worsen the errors we measured, because of a lower count of events.

Bibliography

[1] C.L. Dunford and T.W. Burrows. *Online Nuclear Data Service*. Report **IAEA-NDS-150**, International Atomic Energy Agency, Vienna, Austria.